

Infrared absorption strength and hydrogen content of hydrogenated amorphous silicon

A. A. Langford, M. L. Fleet, and B. P. Nelson

National Renewable Energy Laboratory, 1617 Cole Boulevard, Golden, Colorado 80401

W. A. Lanford

Department of Physics, State University of New York, Albany, New York 12222

N. Maley

Coordinated Science Laboratory, University of Illinois, Urbana, Illinois 61801

(Received 19 August 1991; revised manuscript received 7 February 1992)

We have used infrared transmission and nuclear-reaction analysis to determine the ir absorption strength of the Si-H wagging and stretching modes in hydrogenated amorphous silicon (*a*-Si:H). The films were deposited by plasma-assisted chemical vapor deposition and reactive magnetron sputtering. We show that the widely used ir-data-analysis method of Brodsky, Cardona, and Cuomo can lead to significant errors in determining the absorption coefficients, particularly for films less than $\sim 1 \mu\text{m}$ thick. To eliminate these errors we explicitly take into account the effects of optical interference to analyze our data. We show that the hydrogen content can be determined from the stretching modes at $\omega = 2000$ and 2100 cm^{-1} as well as the wagging mode at $\omega = 640 \text{ cm}^{-1}$. By assigning different oscillator strengths to the 2000- and 2100-cm^{-1} modes, we show that the absorption strength of the stretching modes does not depend on the details of sample preparation, contrary to hypotheses previously invoked to explain experimental data. We obtain $A_{640} = (2.1 \pm 0.2) \times 10^{19} \text{ cm}^{-2}$, $A_{2000} = (9.0 \pm 1.0) \times 10^{19} \text{ cm}^{-2}$, and $A_{2100} = (2.2 \pm 0.2) \times 10^{20} \text{ cm}^{-2}$ for the proportionality constants between the hydrogen concentration and the integrated absorbance of the wagging and stretching modes. The value of A_{640} is $\sim 30\%$ larger than the generally used value. We show that previously published data for both the wagging and stretching modes are consistent with the proportionality factors determined in the present study.

I. INTRODUCTION

The importance of hydrogen to the structural, optical, and electronic properties of hydrogenated amorphous silicon (*a*-Si:H) has led to the development of numerous techniques to measure it. Of these, infrared spectroscopy is perhaps the most widely used since it is nondestructive and easily performed, and yields information about hydrogen content and also the bonding configurations. Infrared spectra of *a*-Si:H consist of three absorption regions¹⁻³—a wagging mode at 640 cm^{-1} , a doublet at $840\text{--}890 \text{ cm}^{-1}$ due to dihydride bending or scissors modes, and two stretching modes centered at ~ 2000 and 2100 cm^{-1} . The 2000-cm^{-1} stretching mode is commonly attributed to isolated monohydrides (SiH) and the 2100-cm^{-1} mode to clustered monohydrides as well as polyhydrides (dihydrides and trihydrides or SiH_x with $x = 2$ or 3).

Infrared absorption for these modes is related to the hydrogen content through the oscillator strengths. The proportionality constant A varies as the inverse of the oscillator strength and relates the hydrogen concentration N_{H} to the integrated absorbance I via

$$N_{\text{H}} = AI, \quad (1)$$

where

$$I = \int (\alpha/\omega) d\omega, \quad (2)$$

α is the absorption coefficient, ω is the frequency in cm^{-1} , and the integral is over the absorption band of interest.² Since attempts to obtain them through theoretical analysis^{2,4} were not very successful, oscillator strengths have been determined empirically by correlating the ir stretching or wagging mode absorbance with H content measured by independent means. For example, ir absorbance has been correlated with nuclear-reaction analysis,⁵⁻¹⁴ hydrogen evolution,^{5,15,16} α particle scattering,^{17,18} secondary ion mass spectrometry (SIMS),^{11,12} and nuclear elastic scattering.^{12,13,19} Most of the studies which measured the wagging-mode absorption support the work of Fang *et al.*,⁵ who found $A_{640} = 1.6 \times 10^{19} \text{ cm}^{-2}$ for the silicon-hydrogen wagging modes. Oguz⁹ and Maley *et al.*¹⁶ reported higher values for A_{640} .

The ir-wagging-mode absorption is proportional to the total hydrogen content independent of the bonding configurations. Absorption at $\sim 840\text{--}890 \text{ cm}^{-1}$ and for the stretching modes, on the other hand, is dependent on the bonding configuration. The proportionality factors for the stretching modes have mostly been derived assuming that the oscillator strength is the same for the 2000- and 2100-cm^{-1} modes.^{5,15,18} Shanks, Jeffrey, and Lowry assigned three different oscillator strengths to the stretching modes of isolated and clustered monohydrides and polyhydrides.²⁰ More recently, Maley *et al.* estimated a proportionality factor for the 2100-cm^{-1} mode based on a correlation with the low-temperature thermal evolution

peaks.¹⁶ These attempts have resulted in widely varying estimates of the proportionality factors for the stretching modes, with several authors suggesting that the oscillator strength depends on the details of sample preparation.^{6,18,21}

Maley and Szafranek²² and Maley²³ have recently shown that the widely used ir-data-analysis method of Brodsky, Cardona, and Cuomo can lead to significant errors in determining the absorption coefficients, particularly for films less than $\sim 1 \mu\text{m}$ thick. Such errors may in part be responsible for the reported variation in the oscillator strengths. In the present study, we explicitly take into account the effects of optical interference to eliminate these errors. We also analyze the ir data by assigning different proportionality factors for the 2000- and 2100- cm^{-1} modes. Using nuclear-reaction analysis as a primary standard we find for *a*-Si:H films grown by plasma-assisted chemical vapor deposition and magnetron sputtering, $A_{640} = (2.1 \pm 0.2) \times 10^{19} \text{ cm}^{-2}$, $A_{2000} = (9.0 \pm 1.0) \times 10^{19} \text{ cm}^{-2}$, and $A_{2100} = (2.2 \pm 0.2) \times 10^{20} \text{ cm}^{-2}$. Much of the previously published data is shown to be consistent with these values, independent of the details of sample preparation.

II. EXPERIMENTAL PROCEDURE

The *a*-Si:H samples were deposited by rf plasma-assisted chemical vapor deposition (PACVD) and reactive dc magnetron sputtering (RMS). Films were deposited simultaneously on double-polished crystalline silicon for ir and nuclear-reaction-analysis (NRA) measurements, and on Corning 7059 glass. Film thicknesses were obtained from profilometric measurements and from the interference fringes for both glass and *c*-Si substrates. Film thicknesses (d) were in the range 0.5–0.75 μm as density measurements by NRA required d to be less than 1 μm . The PACVD films were deposited on the anode of a capacitively coupled parallel plate reactor. The SiH_4 flow was 40 sccm and the pressure was 600 mT for all depositions. The power was 45 mW/cm^2 and the deposition rate was typically 2 $\text{\AA}/\text{s}$. To vary the hydrogen content the substrate heater temperature was varied from 110 to 450°C.

Films were also grown by dc reactive magnetron sputtering in an UHV chamber.^{24,25} The deposition temperature was kept fixed at 230°C and argon partial pressure at 1 mT. The hydrogen content was varied by changing the H_2 partial pressure in the plasma between 0 and 0.8 mT. Table I lists the deposition parameters and thicknesses of both of the RMS and PACVD films used in this study.

Infrared spectra were measured with an IBM 9144 Fourier transform infrared spectrometer and with a Perkin-Elmer 580B dispersive spectrometer. Hydrogen content determined from the two measurements differed by less than 2%. Infrared data are usually analyzed by the method of Brodsky, Cardona, and Cuomo (BCC).² There are two significant sources of error in the BCC method which are described briefly below and in greater detail elsewhere.^{22,23}

In the BCC method, transmission (T) is related to ab-

sorption coefficient (α) via

$$T = 4T_0^2 e^{-\alpha d} / [(1 + T_0)^2 - (1 - T_0)^2 e^{-2\alpha d}], \quad (3)$$

where T_0 is the baseline transmission when $\alpha=0$. The refractive index of *a*-Si:H in ir is a function of the hydrogen content C_H [defined as $100 \times N_H / (N_H + N_{Si})$] and is usually different from that of *c*-Si. This index mismatch at the film-substrate interface gives rise to broad, shallow interference fringes in the transmission spectra. The Si-H absorption bands are superimposed on these fringes, as shown in Fig. 1. In the BCC method, T_0 for the various absorption bands is either taken as the transmission of a bare substrate or is estimated by interpolating the measured transmission from adjacent regions. Both these procedures can lead to significant errors in determining the integrated absorbances. The ir spectra of *a*-Si:H contain a Si-Si stretching mode at 460 cm^{-1} (Ref. 26). Ignoring this in estimating T_0 will result in an underestimate of the integrated absorbance of the 640- cm^{-1} band by as much as 20–30% in some cases. Determining the baseline in the stretching mode region is important for an accurate deconvolution of the 2000- and 2100- cm^{-1} modes. In addition, as we shall see later, the proportionality factors for the stretching modes are larger or, for a given hydrogen content, the absorption bands are weaker (compared to the wagging mode). Thus, uncertainties in estimating the baseline will lead to larger errors in N_H determined from the stretching modes.

The second error in the BCC method leads to a systematic overestimation or underestimation of α in many cases even when the baseline is determined correctly. Unless the films are deposited on roughened *c*-Si substrates, ir absorption is determined by coherent multiple reflections in the film. The BCC method, which is derived for incoherent reflections, overestimates α by up to

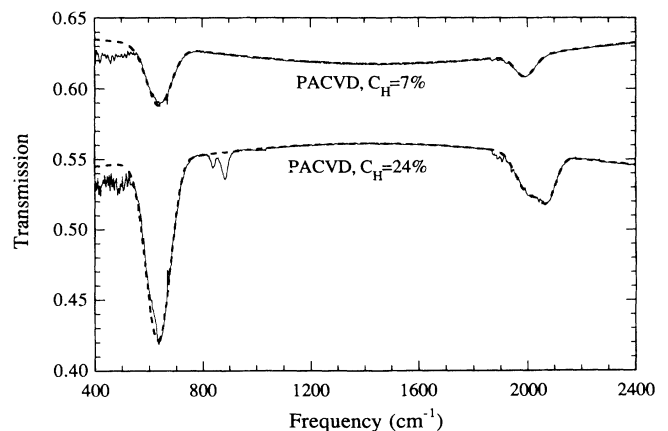


FIG. 1. Transmission spectra of glow-discharge-deposited *a*-Si:H with 7% (upper spectrum) and 24% (lower spectrum) hydrogen. Substrate absorption has been removed by dividing the sample spectra by that of a bare *c*-Si substrate and multiplying by 0.54, which is the transmission of *c*-Si in the nonabsorbing regions. The dashed lines show transmission spectra calculated by taking into account the effects of interference in the film and absorption in the Si-H wagging and stretching modes. The upper spectra have been shifted by 0.1 for clarity.

TABLE I. Deposition parameters and properties of PACVD and magnetron-sputtered samples used in this study.

Temp (°C)	C_H^a	ρ^b	PACVD films							
			d_{mech}^c (μm)	d_{opt}^d (μm)	n^e	I_{640}^f (cm^{-1})	I_{2000}^f (cm^{-1})	I_{2100}^f (cm^{-1})	Δ_{wag}^g (%)	$\Delta_{\text{stretch}}^g$ (%)
110	24.0	0.86	0.54	0.53	3.29	539	44.7	40.5	+38	-13
150	19.8	0.84	0.85	0.85	3.31	473	37.4	29.2	+13	+8
210	13.0	0.82	0.72			343	49.2	10.5	+25	0
270	12.3	0.97	0.58	0.56	3.53	267	43	3.3	+36	-12
270	11.4	0.94	0.58	0.57	3.53	265	43.6	3.2	+36	-12
330	9.6	0.96	0.60	0.58	3.56	233	36	2.1	+34	-10
390	9.5	1.07	0.57	0.59	3.56	196	31.8	1.6	+33	-9
450	7.3	0.93	0.48	0.48	3.58	172	27.9	1.2	+42	-14
Magnetron-sputtered films										
P_{H_2} (mT)										
0	0		0.60	0.60	3.70	0	0	0		
0.1	7.2	0.98	0.56	0.56	3.64	185	29.9	2.8	+36	-12
0.2	14.3	0.99	0.48	0.50	3.54	373	54.4	7.2	+40	-12
0.4	20.2	0.89	0.53			508	61.6	17.5	+33	-8
0.8	29.8	0.86	0.57	0.55	3.34	647	65.2	33.3	+37	-12

^aHydrogen content [$100N_H/(N_H + N_{Si})$] from nuclear reactions.

^bMass density relative to *c*-Si from nuclear reactions.

^cFilm thickness from stylus profilometry.

^dFilm thickness from fitting the fringes.

^eRefractive index from fitting the fringes.

^fIntegrated absorbances determined after converting transmission spectra to absorption spectra using exact equations.

^gPositive and negative numbers, respectively, show the percentage by which the BCC method overestimates and underestimates the integrated absorbance of the wagging and stretching modes.

75% or underestimates it by up to 20%, depending on the film thickness.^{22,23} Using exact equations and known refractive index and absorption coefficient values, Maley and Szafranek²² calculated the transmission of *a*-Si:H on *c*-Si. By analyzing the simulated data, they showed that the two methods most commonly used for ir data reduction [BCC (Ref. 2) and Connell and Lewis²⁷] are equivalent and quantified the errors in them.

The errors in the BCC method are primarily a function of the optical path length, i.e., the product of frequency and film thickness. The errors also depend on the film refractive index and absorption coefficient, although to a lesser extent. For *a*-Si:H films with less than 30 at. % hydrogen, to first order, the absorption spectra determined by the BCC method can be corrected using an empirically determined correction factor

$$\alpha = \alpha_{\text{BCC}} / (1.72 - K\omega d). \quad (4)$$

Here ω is in cm^{-1} , d is in μm , $K = 0.0011$, and the correction is applicable for ωd values for which the denominator is larger than 1. For example, for the wagging mode this correction is required if the film thickness is less than $1 \mu\text{m}$. Equation (4) is a generalization of the correction factor for the 640-cm^{-1} mode given in Ref. 22, and is applicable to all frequencies of interest. Note that this correction is approximate and the errors in α can still be of the order of 10–20%.^{22,23}

To confirm the predicted dependence of the ir absorbance on film thickness, a series of films, $0.1\text{--}2 \mu\text{m}$ thick,

was deposited by PACVD under identical conditions, at a substrate temperature of 250°C , with the deposition time ranging from 8 to 175 min. Figure 2 shows the thickness dependence of the integrated absorbance of the 640- and 2000-cm^{-1} peaks determined by the BCC method. The solid and dashed lines in the figure show the theoretically predicted variation of the absorption coefficient at these two frequencies. As predicted, the apparent absorption determined by the BCC method increases as the film thickness decreases. The apparent increase in absorption

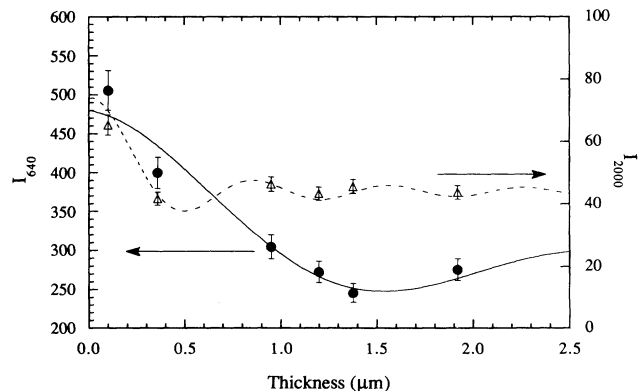
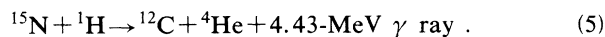


FIG. 2. Thickness dependence of absorption at 640 cm^{-1} (circles and solid line) and 2000 cm^{-1} (triangles and dashed line), which is an artifact of the BCC method. The lines are from a calculation and the points show the experimental data.

also persists to a greater film thickness for the 640-cm^{-1} mode than for the 2000-cm^{-1} mode. The experimental data are in very good agreement with the prediction. In addition, NRA depth profiling shows that the hydrogen content is uniform throughout the films. Thus errors in the BCC method provide a simple explanation for the apparent thickness dependence of hydrogen content determined by ir. This has been observed previously but could not be explained satisfactorily.^{12,13,28}

To eliminate the errors associated with the BCC method in the present study, we have taken optical interference effects into account to convert transmission spectra to absorption spectra. We first fit the measured spectra in the nonabsorbing regions by adjusting the film thickness and refractive index. In the next step the various Si-Si and Si-H absorption bands are fitted with Gaussian peaks. Transmission spectra are calculated by taking into account coherent multiple reflections in the film and incoherent reflections in the substrate. The position, height, and width of each absorption band is adjusted until a good fit is obtained between measured and calculated transmission spectra over the entire frequency range. Figure 1 shows typical fits and Table I shows the film thicknesses and refractive indices obtained by this procedure. A comparison of film thicknesses obtained from fitting the fringes and from stylus profilometry shows very good agreement, except for films whose refractive index is close to the *c*-Si value (3.42). For such films, independent thickness measurements are required since the small fringe amplitude makes it difficult to determine *d* from ir data. Table I also shows the integrated absorbances of the wagging and stretching modes and the errors that would result from the BCC method. Note that the errors, which range between -15% and $+40\%$, are different for the wagging and stretching modes. Also, if uncertainties in estimating the base line are taken into account, the errors in integrated absorbances determined by the BCC method can be even larger.

For an absolute determination of the H content, nuclear-reaction analysis was performed using the reaction



The technique is described briefly here and further details can be found in Ref. 29. The cross section for the γ -ray yield has a very narrow and large resonance for ^{15}N energy of 6.405 MeV. Since nitrogen ions lose some of their energy as they travel through *a*-Si:H the dependence of the γ -ray yield on the energy of the incident ions can be used to obtain the depth profile of hydrogen concentration. The analysis depth is given by

$$x = (E - E_{\text{res}})(dE/dx)^{-1} , \quad (6)$$

where *E* is the incident ion energy, $E_{\text{res}} = 6.405$ MeV, and dE/dx is the rate of energy loss of ^{15}N in the solid. The hydrogen concentration at this depth, $N_{\text{H}}(x)$, is given by

$$N_{\text{H}}(x) = K(dE/dx)N_{\gamma} , \quad (7)$$

where *K* is a constant reflecting the cross section for the reaction of Eq. (5) and the detector efficiency, and N_{γ} is the γ -ray count. Since the stopping power of silicon and hydrogen atoms is a constant, independent of density, the hydrogen profile measurements depend on the ratio $N_{\text{H}}/N_{\text{Si}}$ but not the actual density of atoms. By depth profiling all the way through a film, it is possible to measure the stopping power of the whole film and determine the areal density of atoms. This combined with independent measurements of film thickness, yields the density of the film. In the present set of experiments the film thickness was in the range $0.4\text{--}0.75 \mu\text{m}$, to enable depth profiling into the substrate. Within the depth resolution of the experiment (~ 4 nm at the surface and 40 nm at the film-substrate interface) the hydrogen concentration was found to be uniform throughout the films. The relative uncertainty in the hydrogen concentration is estimated to be $\pm 5\%$. By measuring the ir spectra of films before and after, we have also confirmed that the hydrogen content of the film is unchanged by the NRA measurements. Loss of hydrogen during NRA can be a problem in films of high hydrogen content and low density.⁷

Before presenting the results, we note that hydrogen content is often given as a fraction by dividing N_{H} by 5×10^{22} , the number density of *c*-Si. When quoted as a fraction, it is not clear whether one is referring to the $N_{\text{H}}/N_{\text{Si}}$ ratio or the H mole fraction, i.e., $N_{\text{H}}/(N_{\text{Si}} + N_{\text{H}})$. Obviously, the two values are very different for high hydrogen content. Several groups have measured the mass density of *a*-Si:H as a function of the hydrogen content.^{7,18,19,30-34} In Fig. 3 we convert the mass density to number density, $N_{\text{H}} + N_{\text{Si}}$, and examine its variation with hydrogen content, N_{H} , determined independently. This figure shows that for a large number of films grown and characterized by several different techniques in different laboratories, the number density has an average value of $5.3 \times 10^{22} \text{ cm}^{-3}$, with a rms deviation of 10%. This shows that it is reasonable to specify hydrogen content as a fraction by dividing N_{H} by 5×10^{22} , provided that it is recognized as the mole fraction of hydrogen, $N_{\text{H}}/(N_{\text{H}} + N_{\text{Si}})$.

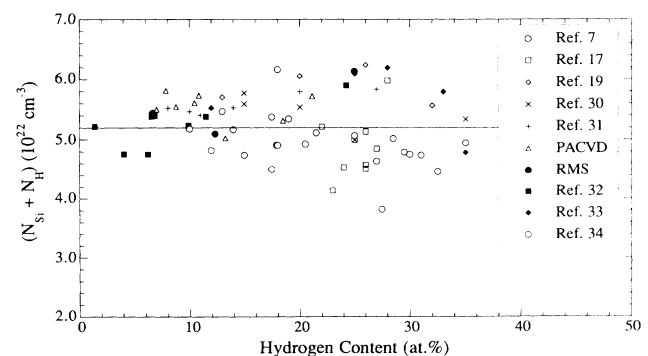


FIG. 3. The dependence of the number density ($N_{\text{Si}} + N_{\text{H}}$) on hydrogen content. The horizontal solid line represents N_{Si} for *c*-Si.

III. RESULTS

A. ir spectra of PACVD and magnetron-sputtered a -Si:H

Figure 4 shows the ir spectra of several a -Si:H samples. The spectra are shown in pairs to compare spectral features for films of similar or nearly similar hydrogen content grown by two different techniques. The hydrogen content, C_H , varies between 7% and 24% for the PACVD samples and between 7% and 30% for the sputtered samples. For films with 7% hydrogen the ir spectra of PACVD and magnetron-sputtered samples are nearly identical. With increasing C_H Fig. 4 reveals interesting differences. The spectra of the magnetron-sputtered material show broader peaks, less absorption in the bending modes at 840–890 cm^{-1} and the stretching mode at 2100 cm^{-1} , and more absorption at 2000 cm^{-1} . Within the experimental uncertainty, the wagging peak can be fit to a single Gaussian for all the films. The 840–890- cm^{-1} doublet is also not as well resolved for the sputtered samples. These broader peaks imply that the amorphous network is slightly more disordered for the sputtered samples (broader bond angle and perhaps bond-length distributions). Some of the spectral differences may also be due to microstructural variations on a larger length scale. It is well known that with increasing hydrogen content PACVD samples show a columnar microstructure.³⁵ Magnetron-sputtered samples deposited at low argon partial pressures, on the other hand, show no columnar features for C_H up to 35%.²⁵ In hydrogen-rich films, columnar microstructure may lead to more hydrogen clustering, as evidenced by the larger 2100- cm^{-1} mode in the PACVD films.

B. Hydrogen content and the Si-H wagging mode

The correlation between N_H , the number of hydrogen atoms in the film, measured by NRA, and the integrated absorbance of the 640 cm^{-1} mode is shown in Fig. 5 for the sputtered and PACVD films. Within the measure-

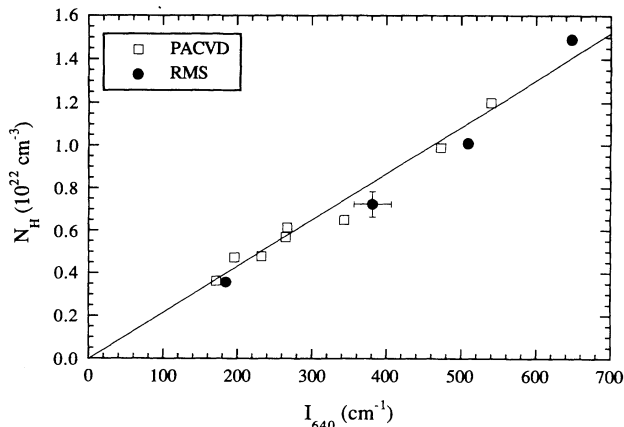


FIG. 5. Hydrogen content (N_H) from NRA vs the integrated absorbance of the 640- cm^{-1} mode for PACVD (squares) and reactive magnetron-sputtered (circles) films. Least-squares fit to the data yields $A_{640} = (2.1 \pm 0.2) \times 10^{19} \text{ cm}^{-2}$.

ment uncertainty, both sets of films show the same trend. A least-squares fit to the data yields a zero intercept and $A_{640} = (2.1 \pm 0.2) \times 10^{19} \text{ cm}^{-2}$. This constitutes the upper limit to A_{640} since infrared absorption is sensitive only to Si-H bonds while NRA measures this component as well as molecular hydrogen. However, we are not aware of any studies which correlate ir absorbance with the amount of hydrogen bonded to Si determined independently (by NMR, for example). Thus, all estimates of A_{640} to date have been obtained by relating ir absorbance to the total hydrogen content. The value of A_{640} obtained in the present study is about 30% larger than the most widely used value of $1.6 \times 10^{19} \text{ cm}^{-2}$ reported by several groups.^{5,6,18} It is in very good agreement with the value of $2.0 \times 10^{19} \text{ cm}^{-2}$ reported by Maley *et al.*¹⁶ and is $\sim 15\%$ smaller than the highest value ($2.5 \times 10^{19} \text{ cm}^{-2}$), reported by Oguz.⁹ These discrepancies in A_{640} can be accounted for by molecular hydrogen provided (i)

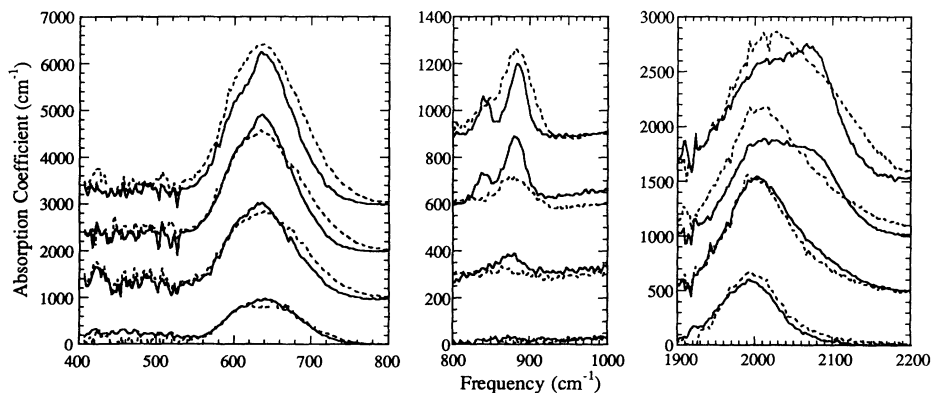


FIG. 4. Absorption spectra of a -Si:H films deposited by PACVD (solid lines) and magnetron sputtering (dashed lines) in the wagging, bending, and stretching-mode regions. Spectra are shown in pairs to compare features for samples with hydrogen content as closely matched as possible. From bottom to top, the hydrogen content is 7%, 13%, 20%, and 24% for PACVD and 7%, 14%, 20%, and 30% for magnetron-sputtered films.

it is a significant fraction of the total hydrogen content and (ii) its amount is the smallest for Refs. 5, 6, and 18, highest for Ref. 9, and in between for the present study. However, we rule out this possibility. Oguz *et al.* did find that their films contained a large amount of inactive hydrogen.^{36,21} However, for magnetron-sputtered films grown under the conditions used in the present study, ir and thermal evolution measurements as a function of annealing show that the molecular hydrogen content is negligible.³⁷

Figure 6 compares the N_H - I_{640} correlation from the present study and from Refs. 5, 6, and 16. This figure includes data for films grown by PACVD, dc magnetron sputtering, and rf diode sputtering, with N_H being determined by NRA or thermal evolution. Figure 6 shows that for $I_{640} < 400 \text{ cm}^{-1}$ all these studies show a similar correlation. For higher I_{640} the data from Refs. 5 and 6 deviate from the rest, leading to a lowering of A_{640} .

We have also examined other previously published results correlating the absorbance of the wagging mode with hydrogen content determined independently.^{10-12,17,18} However, in some cases, the films studied were less than $1 \mu\text{m}$ thick and so the apparent I_{640} is larger than the actual absorbance, as shown in Fig. 2.^{10,12,17,18} Reducing I_{640} to correct for thickness requires a corresponding increase in A_{640} , which brings these reports into agreement with the present findings. Pollock's measurements, for example, show that for films 0.1 – $0.3 \mu\text{m}$ thick the ir analysis, using $A_{640} = 1.6 \times 10^{19} \text{ cm}^{-2}$, agrees with NRA and SIMS while for films 3 – $4 \mu\text{m}$ -thick ir gives H contents which are about 40% lower.¹² For $\sim 1\text{-}\mu\text{m}$ -thick films, Ross *et al.* find that hydrogen content determined from ir with $A_{640} = 1.6 \times 10^{19} \text{ cm}^{-2}$ is lower by as much as 25–35% in comparison with nuclear reactions.¹¹

In short, in view of the discussion in the preceding section, a $\pm 25\%$ uncertainty in the integrated absorbance of the wagging modes is not uncommon if the ir data are analyzed by the BCC (Ref. 2) or the Connell-Lewis²⁷ method. In the absence of a detailed reanalysis of the ir transmission spectra, and given the additional uncertain-

ty in the determination of hydrogen content, we note that all the previously reported correlations between hydrogen content and the wagging-mode absorption are consistent with the value of A_{640} reported in the present study.

C. Hydrogen content and the Si-H stretching modes

While the integrated absorbance of the wagging mode is now widely used as a measure of the total hydrogen content, initial efforts to determine N_H from the ir spectra focused on the Si-H stretching modes at 2000 and 2100 cm^{-1} . The initial attempts to determine the proportionality factor theoretically proved unreliable.^{2,4} Subsequently Freeman and Paul¹⁵ and Fang *et al.*⁵ reported a value of $1.4 \times 10^{20} \text{ cm}^{-2}$ for the stretching-mode proportionality factor by calibrating ir against thermal evolution and/or nuclear reactions. Shanks *et al.* noted that the proportionality factor was material dependent.⁶ For films exhibiting primarily the 2000 - or 2100-cm^{-1} peak, and for films containing fluorine, they observed a different correlation between the stretching-mode absorption and hydrogen content. Other researchers have invoked sample-dependent oscillator strength^{18,21} or the presence of molecular hydrogen¹³ to explain their experimental data. All these studies assumed that the proportionality factor is the same for the 2000 - and 2100-cm^{-1} modes, i.e.,

$$N_H = A_s(I_{2000} + I_{2100}) . \quad (8)$$

In light of the constant oscillator strength of the wagging mode, it is quite puzzling that the proportionality factor for the stretching modes should be so sensitive to the details of film preparation. In fact, if the absorption strength of the stretching modes is sample dependent because of variations in local environment, it would be very surprising if it is the same for both the 2000 - and 2100-cm^{-1} modes. Thus, Eq. (8) may not be appropriate for analyzing the stretching-mode data. It is clear that sample-to-sample variation of oscillator strengths should be invoked only if experimental data cannot be explained satisfactorily by assuming constant and different oscillator strengths for the various Si-H modes. The possibility that the proportionality factor is different for the 2000 - and 2100-cm^{-1} modes has been discussed in the past, but reliable quantitative analysis of experimental data based on this hypothesis has been lacking until recently.^{1,20,21,38}

Shanks, Jeffrey, and Lowry²⁰ assigned three different oscillator strengths for the stretching modes of isolated and clustered monohydrides and polyhydrides. In this case, hydrogen content is related to the stretching-mode absorption via

$$N_H = A_{2000}I_{2000} + A_{2100,\text{SiH}}I_{2100,\text{SiH}} + A_{2100,\text{SiH}_x}I_{2100,\text{SiH}_x} . \quad (9)$$

Since we experimentally only measure N_H , I_{2000} , and I_{2100} ($=I_{2100,\text{SiH}} + I_{2100,\text{SiH}_x}$), it is not possible to determine the three proportionality factors uniquely without further simplifications to Eq. (9). To separate the contributions of polyhydrides and clustered monohydrides to

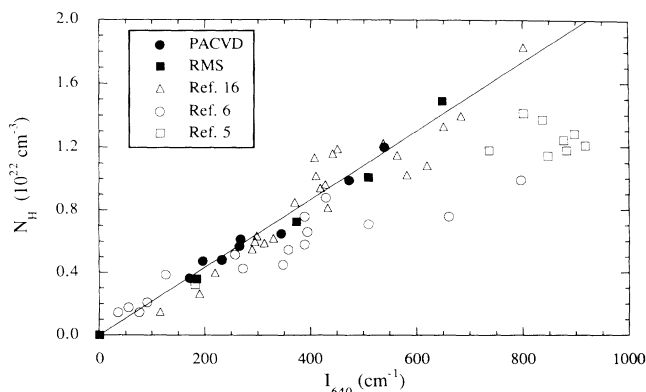


FIG. 6. Hydrogen content (N_H) from NRA or thermal evolution vs the integrated absorbance of the 640-cm^{-1} mode. The line corresponds to $A_{640} = 2.1 \times 10^{19} \text{ cm}^{-2}$.

the 2100-cm⁻¹ mode, Shanks, Jeffrey, and Lowry used films which showed absorption at 2000 and 2100 cm⁻¹ but none at 840–890 cm⁻¹. In the absence of absorption at 840–890 cm⁻¹, which is due to dihydride bending modes, the 2100 cm⁻¹ was attributed to clustered monohydrides. The proportionality factors for isolated and clustered monohydrides were then obtained from Eq. (9) with $I_{2100, \text{SiH}_x} = 0$. Next, using films which showed bending modes, and assuming that the contribution of clustered monohydrides to the 2100-cm⁻¹ mode was constant, they estimated a proportionality factor for the polyhydride stretching and bending modes. However, since this study was based on a limited number of samples, these proportionality factors have large uncertainty¹ and the analysis also presents two problems. First, there is no physical justification provided for the assumption that the concentration of clustered monohydrides remains constant while the total hydrogen content is varied. In fact, the clustered hydrogen phase has been associated with the internal surfaces of microvoids and small-angle x-ray-scattering measurements show that the microvoid density increases with C_{H} .³⁹ Second, as discussed in the next section, the dynamic charge associated with the proportionality factor derived for the 2000-cm⁻¹ mode is too large and inconsistent with the observed frequency shift of isolated monohydrides.

In the present study we start with Eq. (9), i.e., we assign three different oscillator strengths to the stretching modes of isolated and clustered monohydrides and polyhydrides. Recently, Lucovsky *et al.* have shown that hydrogen bonding configurations in *a*-Si:H are determined by a random distribution of hydrogen among available sites.⁴⁰ In this limit the concentrations of polyhydrides and clustered monohydrides are approximately proportional to each other.⁴¹ This implies that

$$I_{2100, \text{SiH}} = KI_{2100, \text{SiH}_x} \quad (10)$$

With this, Eq. (9) can be written as

$$N_{\text{H}} = A_{2000}I_{2000} + A_{2100}I_{2100} \quad (11)$$

where A_{2100} is a single effective proportionality factor for the 2100-cm⁻¹ mode. It is a weighted average of $A_{2100, \text{SiH}}$ and A_{2100, SiH_x} and is given by

$$A_{2100} = (KA_{2100, \text{SiH}} + A_{2100, \text{SiH}_x}) / (K + 1) \quad (12)$$

We have analyzed the data from the present study and Ref. 16, assuming that A_{2000} and A_{2100} are different and do not depend on the details of sample preparation. Using N_{H} determined by NRA or thermal evolution, multivariate regression analysis of Eq. (11) yields $A_{2000} = (9.0 \pm 1.0) \times 10^{19}$ cm⁻² and $A_{2100} = (2.2 \pm 0.2) \times 10^{20}$ cm⁻². Recently, Amato *et al.* correlated the stretching-mode absorption with N_{H} determined by elastic recoil detection for *a*-Si:H samples grown by low-pressure chemical vapor deposition.³⁸ They obtained $A_{2000} = (7.3 \pm 1.0) \times 10^{19}$ cm⁻² and $A_{2100} = (2.1 \pm 0.15) \times 10^{20}$ cm⁻², which are in excellent agreement with our values.

Figure 7 compares N_{H} determined from the integrated

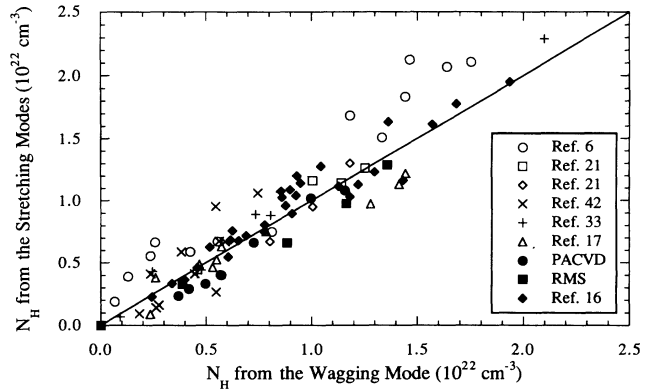


FIG. 7. Correlation between N_{H} determined from the integrated absorbance of the stretching modes and the wagging mode using the proportionality factors determined in this study. The solid line represents $N_{\text{H}}(\text{stretch}) = N_{\text{H}}(\text{wag})$.

absorbance of the wagging and stretching modes using $A_{2000} = (9.0 \pm 1.0) \times 10^{19}$ cm⁻², $A_{2100} = (2.2 \pm 0.2) \times 10^{20}$ cm⁻², and $A_{640} = 2.1 \times 10^{19}$ cm⁻². To check the validity of these proportionality factors, we have analyzed some of the previously published data on stretching and wagging modes.^{6,16,17,21,33,42} These are also shown in Fig. 7. Note that to first order there is reasonably good agreement between N_{H} determined from the stretching and wagging modes for a wide range of samples.

There is some scatter in the data in Fig. 7, which is most probably due to errors in data analysis. As described in Sec. II, uncertainties in estimating the baseline and thickness-dependent artifacts are two significant sources of error in ir data reduction by the BCC method. Table I, for example, shows that for a 0.5- μm -thick film the BCC method overestimates α for the wagging mode by $\sim 40\%$ and underestimates α for the stretching modes by $\sim 15\%$. At a thickness of $\sim 1.5 \mu\text{m}$, on the other hand, α is underestimated by $\sim 20\%$ for the wagging mode and overestimated by $\sim 12\%$ for the stretching modes.²³ If we also take into account measurement accuracy and uncertainty in estimating the baseline and deconvoluting the stretching modes, we see that the errors in integrated absorbance can cancel out in some cases or add up and be $\geq 25\%$ in other cases. Such errors can be reduced considerably by using exact equations. However, it is not possible to do this for most of the previously published data, and within this error Fig. 7 shows that there is good agreement between N_{H} from the wagging and stretching modes. For the samples from the present study and Ref. 16, for which the experimental errors are smaller, we do see that there is a stronger correlation between N_{H} from the wagging and stretching modes. We have noted earlier that, for a given hydrogen content, the ir spectra of PACVD and magnetron-sputtered films show some differences (Fig. 4 and Sec. III A). It is interesting to note that, despite these differences, the correlation between the integrated absorbances of the wagging and stretching modes is similar for the two sets of films.

IV. DISCUSSION

In this section we discuss the results from the present study in view of the existing experimental and theoretical understanding of infrared absorption in *a*-Si and *a*-Si:H.

A. Hydrogen content, bonding configurations, and microvoids

The stretching-mode proportionality factor in Refs. 5 and 15 ($1.4 \times 10^{20} \text{ cm}^{-2}$) is approximately equal to the average of A_{2000} and A_{2100} . As a consequence, in samples where the 2000- and 2100- cm^{-1} modes are of comparable intensity, the total hydrogen content determined from the stretching modes is similar for the two choices of the proportionality factors. However, using a single proportionality factor for the two peaks will lead to an overestimate of N_{H} for the 2000- cm^{-1} mode and an underestimate for the 2100- cm^{-1} mode. At low hydrogen contents, where the 2000 cm^{-1} dominates, we find that $A_{2000} = 9.0 \times 10^{19} \text{ cm}^{-2}$ yields results that are more consistent with the wagging mode. The results of Shanks *et al.* (see Fig. 1 in Ref. 6) are also consistent with this observation.

Accurate and quantitative information about hydrogen bonding configurations is important in understanding the structure of the amorphous network. For example, *a*-Si:H is known to have microvoids, on whose internal surfaces hydrogen is believed to cluster. Mahan *et al.* have used small-angle x-ray scattering (SAXS) to determine the number and size of the microvoids.^{39,43} They also correlated SAXS with ir to determine the degree of hydrogenation of the internal surfaces. However, to determine the amount of hydrogen in the microvoids, they either scaled the hydrogen content from the wagging mode by the relative area of the 2100- cm^{-1} mode [$=I_{2100}/(I_{2000} + I_{2100})$] or used $A_{2100} = 1.4 \times 10^{20} \text{ cm}^{-2}$. Based on our results, both methods will underestimate the amount of hydrogen in the 2100- cm^{-1} mode and thus overestimate the degree of Si-Si bond reconstruction on the internal surfaces of microvoids. Quantitative understanding of this issue is important because hydrogen motion on the internal surfaces of microvoids has been proposed as a possible mechanism for carrier-recombination-induced defect creation in *a*-Si:H.⁴⁴

B. ir absorption and the static and dynamic dipole moments of Si-H bonds

In the preceding section we have described the relationship between ir absorption and hydrogen content in terms of the proportionality factors A_{640} , A_{2000} , and A_{2100} . These vary as the inverse of the absorption strength and are related to e^* , the effective charge of the dipole via the relation

$$A = cn\mu\omega/2\pi^2e^{*2}, \quad (13)$$

where c is the speed of light, n is the refractive index, and μ is the reduced mass.¹ The refractive index of *a*-Si:H is a function of the hydrogen content. For magnetron-sputtered films, for example, n is ~ 3.7 for unhydrogenat-

ed *a*-Si and decreases to ~ 3.2 for films with 30% hydrogen.²³ However, to be consistent with the existing literature we use $n = 3.42$, the value for *c*-Si. The proportionality factors of the present study yield $e^* = 0.47, 0.39,$ and 0.26 (in units of electron charge) for the 640-, 2000-, and 2100- cm^{-1} bands, respectively. Taking the variation in the refractive index with hydrogen content into account will lead to a slight lowering of the e^* values. For comparison, the data of Shanks, Jeffrey, and Lowry²⁰ correspond to $e^* = 0.53, 0.8, 0.4,$ and 0.24 for the 640-, 2000-, 2100- (clustered monohydrides), and 2100- cm^{-1} (polyhydrides) bands, respectively.

For the isolated monohydrides, Shanks *et al.*⁶ and Cardona¹ have argued that the stretching frequency is shifted from 2100 down to 2000 cm^{-1} by the depolarizing field produced by a vibrating dipole in a cavity. The frequency shift $\Delta\omega$ depends on the effective charge e^* via

$$\Delta\omega = -e^{*2}/2mR^3\omega[(\epsilon - 1)/(2\epsilon + 1)], \quad (14)$$

where ϵ is the film dielectric constant and R is the radius of the cavity.¹ Cardona finds that the observed frequency shift of $\sim 100 \text{ cm}^{-1}$ corresponds to $e^* = 0.4$. This is in excellent agreement with the value obtained from A_{2000} in the present study and Ref. 38. In contrast, the e^* value of Shanks, Jeffrey, and Lowry²⁰ predicts a frequency shift nearly four times larger than the observed value.

Connell and Pawlik⁴ and Brodsky, Cardona, and Cuomo² have attempted to explain the infrared absorption strength of *a*-Si:H by starting with the e^* values of gaseous silanes and incorporating local-field corrections due to the dielectric screening in a solid. However, obtaining a fundamental understanding of ir absorption in *a*-Si:H requires a more rigorous approach since local-field corrections do not take into account the effects of network distortions. In general, infrared absorption by a vibrational mode arises from the dipole moment of a bond, which in turn is due to static or dynamic charge transfer between the atoms. The static charge (e_s^*) arises from the difference in the electronegativities of the atoms and the dynamic term (e_d^*) from changes in the charge distribution as the atoms vibrate. For unhydrogenated *a*-Si Winer and Cardona⁴⁵ have shown that the static terms are negligible and that ir absorption arises from charge transfer due to phonon-induced bond-angle and bond-length distortions. The ir absorption spectrum of *a*-Si does not simply mimic the phonon spectrum—the relative intensities of the TA-, LA-, LO-, and TO-like peaks are quite different in the two spectra. It is thus interesting to note that Winer and Cardona obtained excellent agreement between theory and experiment over the entire spectral range by taking the effects of local distortions into account and using a single value for the dynamic charge ($e_d^* = 0.44$). It is also interesting to note that the e^* values obtained in the present study for the 640- and 2000- cm^{-1} modes in *a*-Si:H are comparable to the e^* of *a*-Si. A semiempirical theoretical approach similar to that of Winer and Cardona would clearly be very useful in obtaining a better understanding of ir absorption in *a*-Si:H.

The relative contributions of the static and dynamic terms to the ir activity of *a*-Si:H are not yet known.

From the electronegativity difference (1.8 for Si and 2.1 for H) we get $e_s^* = 0.05$ for the static charge of an isolated Si-H bond.⁴⁶ From photoemission experiments, Ley, Reichardt, and Johnson,⁴⁷ on the other hand, estimate $e_s^* = 0.15$ for Si-H bonds in *a*-Si:H. If interference between the static and dynamic dipole moments is negligible, even with the higher value for e_s^* , the static mechanism might account for only $\sim 10\%$ of the ir absorption for the 640- and 2000- cm^{-1} modes. On the other hand, the static term might be significant for polyhydride and/or clustered monohydride stretching modes.

The static mechanism may also be important for all the modes in some alloys. For example, the absorption strength of Si-H stretch modes in *a*-Si,C:H alloys has been shown to be a function of carbon content.⁴⁸ This has been attributed to a static charge transfer from Si to the more electronegative C in C-Si-H configurations, and an accompanying increase in the dipole moment of Si-H bonds. A similar effect might be expected in *a*-Si:H:F alloys also since F is even more electronegative than C. Figure 7 includes data from Langford *et al.*⁴² for *a*-Si:H:F alloys with up to 7% F. It is interesting to note that there is a good correlation between N_H determined from the stretching and wagging modes. This may be due to only a small number of Si atoms being bonded to both F and H. Another possibility is that the addition of F enhances the ir activity of both the wagging and stretching modes. Independent measurements of H content in these films would be useful to see if the proportionality factors determined for *a*-Si:H are valid for the fluorinated films as well.

C. Variability of the Si-H oscillator strengths

One of the strongest arguments for the variability of the oscillator strength comes from Oguz *et al.*²¹ They found a large increase in the intensity of the 840- and 2000- cm^{-1} modes ($\sim 175\%$ and 55% , respectively) in *a*-Si:H films bombarded by 100 or 200 keV He^+ ions and much smaller or no change in the 640-, 890-, and 2100- cm^{-1} modes. These changes in the ir spectra were reversible with annealing at 320 °C. Oguz *et al.* concluded that defects produced in the vicinity of Si-H bonds by He^+ ion bombardment selectively increase the oscillator strength of the 840- and 2000- cm^{-1} modes. They also suggested that variations in defect structures (dangling bonds or weak bonds) in films grown by different methods and under different conditions would lead to the ir oscillator strengths being sample dependent. In examining the data of Oguz *et al.*, two points are worth noting.

The explanation of Oguz *et al.* that the oscillator strengths of the 840- and 2000- cm^{-1} modes are very sensitive to the local environment might be correct. Even if this is true, we note that the ion energies and fluences used in their experiment lead to considerable disorder through the formation of a large number of weak and dangling bonds. This represents an extreme condition which is not representative of typical films. For example, *a*-Si:H films usually have 10^{15} – 10^{17} dangling bonds/ cm^3 . Helium-ion bombardment, in comparison, produces $\sim 10^{20}$ dangling bonds/ cm^3 .⁴⁹ Even if a dangling bond on

or near a Si-H bond increases its oscillator strength, it is clear that it will not have a measurable effect on the ir spectra of typical films.

In interpreting their ion bombardment results, Oguz *et al.* ruled out the possibility of the changes in ir reflecting changes in Si-H bonding configurations. We have used TRIM simulations to examine the consequences of bombarding *a*-Si:H with 200-keV He^+ ions.⁵⁰ For a 6000-Å-thick film with $\sim 30\%$ hydrogen and a He^+ -ion fluence of 10^{16} cm^{-2} (which are the parameters from Ref. 21), TRIM simulations show that $\sim 10^{22}$ Si atoms/ cm^3 and 10^{21} H atoms/ cm^3 are displaced from their original positions. From the ir spectra of the as-deposited films, we estimate $N_H = 2.2 \times 10^{21}$ and 1.0×10^{22} for the 2000- and 2100- cm^{-1} modes, respectively, and that at least 18% of the Si atoms are bonded to H atoms.⁵¹ Given this information, it is not clear that we can rule out changes in hydrogen bonding configurations upon bombardment. Stein and Peercy⁵² have observed a conversion of polyhydride sites to monohydride sites in *a*-Si:H bombarded by He ions. In fact, the changes observed by Oguz *et al.* are qualitatively consistent with what is expected from the TRIM simulations: given the larger concentration of hydrogen in the 2100- cm^{-1} mode prior to bombardment, a small net shift of hydrogen from this mode to 2000 cm^{-1} is probable. Due to its large oscillator strength, this will give rise to a large increase in the 2000- cm^{-1} mode. The data from Oguz *et al.* are included in Fig. 7. This figure shows that, despite the large increase in the area of the 2000- cm^{-1} mode upon bombardment, there is good agreement between the hydrogen contents determined from the wagging and stretching modes.

Finally, for the sake of argument, we can ignore experimental errors and say that the scatter in Fig. 7 is due to a sample-to-sample variation of the oscillator strengths. However, this is not the only explanation. As we noted earlier, the value of A_{2100} determined in the present study is a weighted average of $A_{2100, \text{SiH}}$ and A_{2100, SiH_x} [see Eq. (12)]. If hydrogen bonding is nonrandom, then the ratio of polyhydride to clustered monohydride concentration and hence the factor K in Eqs. (10) and (12) may vary from sample to sample. In this case A_{2100} can be sample dependent even if the oscillator strengths for the isolated and clustered monohydrides and polyhydrides are constant (provided that $A_{2100, \text{SiH}} \neq A_{2100, \text{SiH}_x}$). Further theoretical and experimental studies are in progress to understand the nature of Si-H bonding and to determine whether the oscillator strengths of various Si-H modes are sample dependent.

V. SUMMARY

We have used nuclear-reaction analysis (NRA) to determine the absorption strength of the Si-H wagging and stretching modes in *a*-Si:H deposited by PACVD and magnetron sputtering. We have shown that converting transmission spectra to absorption spectra by the most commonly used method of Brodsky, Cardona, and Cuomo leads to significant errors in α , particularly in films less than ~ 1 μm thick. We have eliminated these errors

by taking into account the effects of optical interference in our data analysis.

By comparing ir and NRA, we have determined the proportionality factors between hydrogen content and the integrated absorbance of the Si-H wagging and stretching modes. We obtain $A_{640} = (2.1 \pm 0.2) \times 10^{19} \text{ cm}^{-2}$ as the proportionality factor for the wagging mode. Previous estimates for this parameter have ranged from 1.6×10^{19} to $2.5 \times 10^{19} \text{ cm}^{-2}$, most probably due to uncertainties in ir data reduction. Assuming random hydrogen bonding we have determined the proportionality factors for the stretching modes. These are $A_{2000} = (9.0 \pm 1.0) \times 10^{19} \text{ cm}^{-2}$ and $A_{2100} = (2.2 \pm 0.2) \times 10^{20} \text{ cm}^{-2}$, where A_{2100} is a weighted average of the proportionality factors for polyhydrides and clustered monohydrides. In contrast with many previously pub-

lished reports, these values are found to be independent of the details of sample preparation. Within the accuracy of the BCC method, a large body of previously published data for both the wagging and stretching modes is shown to be consistent with the proportionality factors determined in the presented study.

ACKNOWLEDGMENTS

The work at the University of Illinois was supported by the Thin Film Solar Cell Program of the Electric Power Research Institute under Contract Nos. EPRI RP 2824-1 and EPRI RP 8001-7. The work at NREL is supported by U.S. DOE under Contract No. DE-AC02-83CH-10093. The authors are grateful to Dr. Richard Crandall for stimulating this study.

- ¹M. Cardona, *Phys. Status Solidi B* **118**, 463 (1983).
- ²M. H. Brodsky, M. Cardona, and J. J. Cuomo, *Phys. Rev. B* **16**, 3556 (1977).
- ³G. Lucovsky, R. J. Nemanich, and J. C. Knights, *Phys. Rev. B* **19**, 2064 (1979).
- ⁴G. A. N. Connell and J. R. Pawlik, *Phys. Rev. B* **13**, 787 (1976).
- ⁵C. J. Fang, K. J. Gruntz, L. Ley, M. Cardona, F. J. Demond, G. Müller, and S. Kalbitzer, *J. Non-Cryst. Solids* **35&36**, 255 (1980).
- ⁶H. Shanks, C. J. Fang, L. Ley, M. Cardona, F. J. Demond, and S. Kalbitzer, *Phys. Status Solidi B* **100**, 43 (1980).
- ⁷M. H. Brodsky, M. A. Frisch, J. F. Ziegler, and W. A. Lanford, *Appl. Phys. Lett.* **30**, 561 (1977).
- ⁸J. C. Bruyère, A. Deneuve, A. Mini, J. Fontenille, and R. Danielou, *J. Appl. Phys.* **51**, 2199 (1980).
- ⁹S. Oguz, Ph.D. thesis, Harvard University, 1981. Oguz determined a proportionality factor between N_H and $\int \alpha dE$. We have converted this into a proportionality factor between N_H and $\int (\alpha/\omega) d\omega$, which is the more commonly used form.
- ¹⁰S. Al Dallal, S. Kalem, J. Bourneix, J. Chevallier, and M. Toulemonde, *Philos. Mag. B* **50**, 493 (1984).
- ¹¹R. C. Ross, I. S. T. Tsong, and R. Messier, *J. Vac. Sci. Technol.* **20**, 406 (1982).
- ¹²G. A. Pollock, in *Applied Material Characterization*, edited by W. Katz and P. Williams, MRS Symposia Proceedings No. 48 (Materials Research Society, Pittsburgh, 1985), p. 379.
- ¹³J. F. Currie, P. Depelsenaire, S. Galarneau, J. L'Ecuyer, R. Groleau, J. C. Bruyère, and A. Deneuve, *J. Phys. (Paris)* **42**, L373 (1981).
- ¹⁴S. H. Sie, D. R. McKenzie, and G. B. Smith, *Appl. Surf. Sci.* **22/23**, 908 (1985).
- ¹⁵E. C. Freeman and W. Paul, *Phys. Rev. B* **18**, 4288 (1978).
- ¹⁶N. Maley, A. Myers, M. Pinarbasi, D. Leet, J. R. Abelson, and J. A. Thornton, *J. Vac. Sci. Technol. A* **7**, 1267 (1989).
- ¹⁷P. John, I. M. Odeh, M. J. K. Thomas, M. J. Tricker, and J. I. B. Wilson, *Phys. Status Solidi B* **104**, 607 (1981).
- ¹⁸P. John, I. M. Odeh, M. J. K. Thomas, M. J. Tricker, J. I. B. Wilson, J. B. A. England, and D. Newton, *J. Phys. C* **14**, 309 (1981).
- ¹⁹T. Imura and A. Hiraki, in *Semiconductor Technologies*, Japan Annual Reviews in Electronics, Computers & Telecommunications, Vol. 8, edited by J. Nishizawa (North-Holland, Amsterdam, 1983), p. 155.
- ²⁰H. R. Shanks, F. R. Jeffrey, and M. E. Lowry, *J. Phys. (Paris) Colloq.* **42**, C4-773 (1981).
- ²¹S. Oguz, D. A. Anderson, W. Paul, and H. J. Stein, *Phys. Rev. B* **22**, 880 (1980).
- ²²N. Maley and I. Szafrank, in *Amorphous Silicon Technology*, edited by P. C. Taylor, M. J. Thompson, P. G. LeComber, Y. Hamakawa, and A. Madan, MRS Symposia Proceedings No. 192 (Materials Research Society, Pittsburgh, 1990), p. 663.
- ²³N. Maley (unpublished).
- ²⁴M. Pinarbasi, A. M. Myers, D. Leet, L. H. Chou, N. Maley, and J. A. Thornton, *Superlatt. Microstruct.* **3**, 331 (1987).
- ²⁵M. Pinarbasi, N. Maley, M. J. Kushner, A. M. Myers, J. R. Abelson, and J. A. Thornton, *J. Vac. Sci. Technol. A* **7**, 1210 (1989).
- ²⁶S. C. Shen, C. J. Fang, M. Cardona, and L. Genzel, *Phys. Rev. B* **22**, 2913 (1980).
- ²⁷G. A. N. Connell and A. Lewis, *Phys. Status Solidi B* **60**, 291 (1973).
- ²⁸S. Hasegawa and Y. Imai, *Philos. Mag. B* **46**, 239 (1982).
- ²⁹W. A. Lanford, *Solar Cells* **2**, 351 (1980).
- ³⁰M. Grimsditch, W. Senn, G. Winterling, and M. H. Brodsky, *Solid State Commun.* **26**, 229 (1978).
- ³¹H. Fritzsche, M. Tanielian, C. C. Tsai, and P. J. Gaczi, *J. Appl. Phys.* **50**, 3366 (1979).
- ³²A. H. Mahan (unpublished).
- ³³J. C. Knights, in *Structure and Excitations of Amorphous Solids*, edited by G. Lucovsky and F. L. Galeener, AIP Conf. Proc. No. 31 (AIP, New York, 1976), p. 296.
- ³⁴H. Meiling, M. J. Van Den Boogaard, R. E. I. Schropp, J. Bezemer, and W. F. Van Der Weg, in *Amorphous Silicon Technology* (Ref. 22), p. 645.
- ³⁵J. C. Knights and R. A. Lujan, *Appl. Phys. Lett.* **35**, 244 (1979).
- ³⁶S. Oguz, R. W. Collins, M. A. Paesler, and W. Paul, *J. Non-Cryst. Solids* **35-36**, 231 (1980).
- ³⁷N. Maley (unpublished data).
- ³⁸G. Amato, G. Della Mea, F. Fizzotti, C. Manfredotti, R. Marchiso, and A. Paccagnella, *Phys. Rev. B* **43**, 6627 (1991).
- ³⁹A. H. Mahan, D. L. Williamson, B. P. Nelson, and R. S. Crandall, *Solar Cells* **27**, 465 (1989).
- ⁴⁰G. Lucovsky, G. N. Parsons, C. Wang, B. N. Davidson, and D. V. Tsu, *Solar Cells* **27**, 121 (1989); G. Lucovsky, B. N. Davidson, G. N. Parsons, and C. Wang, *J. Non-Cryst. Solids* **114**, 154 (1989).
- ⁴¹It is possible to show this using a probabilistic argument—in

- a*-Si:H the dangling-bond concentration is small enough ($\leq 10^{16} \text{ cm}^{-3}$) that we can consider all Si atoms to be fourfold coordinated. Then, if x is the hydrogen content, SiH₂ and SiH₃ concentrations vary as $x^2(1-x)^3$ and $x^3(1-x)^2$, respectively. We consider a monohydride to be isolated if the n nearest neighbors of a H are all Si atoms, i.e., the isolated monohydride content varies as $x(1-x)^n$. We do not know of a well-defined value for n , but for $n \geq 4$ a plot of polyhydride versus clustered monohydride concentration shows a nearly linear relationship for hydrogen contents up to 30–35 %.
- ⁴²A. A. Langford, A. H. Mahan, M. L. Fleet, and J. Bender, *Phys. Rev. B* **41**, 8359 (1990), and unpublished data.
- ⁴³A. H. Mahan, D. L. Williamson, B. P. Nelson, and R. S. Crandall, *Phys. Rev. B* **40**, 12 024 (1989).
- ⁴⁴D. E. Carlson, in *Materials Issues in Amorphous Semiconductor Technology*, edited by D. Adler, Y. Hamakawa, and A. Madan, MRS Symposia Proceedings No. 70 (Materials Research Society, Pittsburgh, 1986), p. 467.
- ⁴⁵K. Winer and M. Cardona, *Solid State Commun.* **60**, 207 (1986).
- ⁴⁶L. Pauling, *The Nature of the Chemical Bond* (Cornell University Press, Ithaca, NY, 1960).
- ⁴⁷L. Ley, J. Reichardt, and R. L. Johnson, *Phys. Rev. Lett.* **49**, 1664 (1982).
- ⁴⁸H. Wieder, M. Cardona, and C. R. Guarnieri, *Phys. Status Solidi B* **92**, 99 (1979).
- ⁴⁹J. S. Payson and J. R. Woodyard, in *Conference Record of Twentieth IEEE Photovoltaic Specialists* (IEEE, New York, 1988), p. 990.
- ⁵⁰J. F. Ziegler, J. P. Biersack, and U. Littmark, *The Stopping and Range of Ions in Solids* (Pergamon, New York, 1985). The simulations were done using TRIM code version 5.2.
- ⁵¹We take $N_{\text{Si}} = 3.8 \times 10^{22} \text{ cm}^{-3}$ so that $N_{\text{H}} + N_{\text{Si}} = 5 \times 10^{22} \text{ cm}^{-3}$. The number of Si atoms bonded to H is 2.2×10^{21} and $5 \times 10^{21} \text{ cm}^{-3}$ for the 2000- and 2100-cm⁻¹ modes, respectively, if we assume that the 2100 cm⁻¹ is only due to dihydrides. This corresponds to ~18% of the Si atoms being bonded to H atoms.
- ⁵²H. J. Stein and P. S. Peercy, *Appl. Phys. Lett.* **34**, 604 (1979).